Effect of High Solid Concentration on Friction in a Transitional and Turbulent Flow of Bioliquid Suspension

ARTUR S. BARTOSIK
Department of Production Engineering,
Kielce University of Technology,
Al. Tysiaclecia P.P. 7, 25-314, Kielce,
POLAND

Abstract: Some suspensions in nature have a complex structure and demonstrate a yield shear stress and a non-linear relationship between the shear rate and the shear stress. Kaolin clay suspension is such an example in engineering, whereas in nature it is blood. This study represents an innovative approach to simulate bioliquid flow, similar to that of blood when the solid concentration is high. The objective of this study is to examine the influence of high solid concentration of bioliquid, similar to blood, on energy losses and velocity profiles in turbulent and transitional flow in a narrow tube. Using the analogy between the suspension of kaolin clay and blood, the physical model and the mathematical model were formulated. The mathematical model comprises continuity and time-averaged momentum equations, a two-equation turbulence model for low Reynolds numbers, and a specially developed wall damping function, as such suspensions demonstrate the damping of turbulence. Experimental data on blood rheology for solid concentrations equal to 43% and 70% by volume, gathered from the literature, were used to establish a rheological model. The results of the simulations indicated that an increase of solid concentration in bioliquid suspension from 43% to 70% causes an increase in wall shear stress to approximately 10% and 6% for transitional and turbulent flow, respectively, and changes in velocity profiles. Such simulations are important if an inserted stent or a chemical additive to the bioliquid suspension is considered, as they can influence the shear stress. The results of the simulations are presented in graphs, discussed, and conclusions are formulated.

Key-Words: Turbulent and transitional flow; suspension similar to blood; damping of turbulence, non-Newtonian suspension; blood friction.

Received: October 8, 2022. Revised: March 8, 2023. Accepted: April 12, 2022. Published: May 18, 2023.

1 Introduction

Solid particles suspended in a liquid can have different densities, shapes, degradation during movement, and a tendency to settle. The mixture of liquid and fine solid particles with a diameter of a few microns is named ‘suspension’. It is common for suspensions to exhibit a nonlinear relationship between shear stress and shear rate, and this depends mainly on the concentration of solid particles in liquid and the properties of both phases, [1].

An example of a suspension, which exists widely in nature, is kaolin clay. Kaolin clay includes solid particles such as kaolinite, quartz, mica, and water as a carrier liquid, [2]. An example of a bioliquid suspension is blood. The solid phase of human blood constitutes cellular elements, usually more than 30% by volume. There are three types of cellular elements, for example, red blood cells (erythrocytes), white blood cells (leukocytes), and platelets. Erythrocytes play a dominant role, since they contribute approximately 99% of all cellular elements, [3], [4], [5]. Erythrocytes have a shape similar to a disc with a diameter of approximately 7 μm and a thickness of approximately 2 μm and are responsible for the transport of oxygen and carbon dioxide, [6], [7], [8], [9]. Erythrocytes contribute significantly to blood viscosity and strongly affect blood rheology, [10]. The carrier liquid of cellular elements in the blood is named plasma. Plasma is a Newtonian liquid with a density and viscosity similar to water because it contains about 90% of water, [3].

When analysing predictions of bioliquid flow, such as blood, in an aorta, one can mention the research of [11], who considered a one-dimensional numerical model, and, [12], who considered a two-dimensional numerical model. They used the Casson rheological model; however, their studies focused only on laminar flow. Some researchers have used turbulent models to predict wall shear stress and energy losses in an aorta. For example,

[13] used the large eddy simulation (LES) and the model of the normalised group k-ε (RNG k-ε). The authors assumed that the suspension is Newtonian and made simulations only for a moderate concentration of erythrocytes, [13].

Available studies on transitional and turbulent blood flow are very rare because the dominant flow in vessels is laminar. However, during intensive physical exercises or the deceleration phase of the blood flow, a transient or turbulent flow can appear, [14], [15]. No studies were found that dealt with the influence of a high solid concentration of erythrocytes on frictional losses in transitional or turbulent blood flows. Most studies consider laminar blood flow or treat the blood as a Newtonian liquid and consider the erythrocyte concentration below 45% by volume, [16]. The laminar flow is easier to model compared to a transitional or turbulent one. Therefore, this study presents modeling and simulations of a transitional or turbulent bioliquid flow, similar to blood, with a high solid concentration. The motivation to use such a high solid concentration comes from the literature. Available studies indicated that a high concentration of erythrocyte count symptoms can include shortness of breath, fatigue, headaches, or during intense exercises, [17], [18], [19].

Considering bioliquids, similar to blood suspensions, and Kaolin clay suspensions, we can find a similarity between them. For instance, both suspensions have a similar size and shape of solid particles and tend to form rouleaux at a low shear rate, causing an increase in yield shear stress and viscosity, [20], [21]. When the shear rate increases, the erythrocyte rouleaux become progressively disassociated. The term rouleaux (singular: rouleau) indicates stacks or aggregation of erythrocyte cells in blood, [22]. In the case of kaolin clay suspension, such an aggregation is called a 'flocculation', [23], [24].

Experiments with *in vivo* blood flow are very difficult. The wall shear stress can be directly estimated from phase contrast (PC) in magnetic resonance (MR) measurements of blood velocity. However, the exact position of the flow domain (vessel) is not known because it moves when the pump (heart) is working. Even a small error in boundary identification significantly influences the measurements. For this reason, we still face difficulties in accessing reliable measurements of blood friction. Such measurements are essential for the validation of mathematical models. Several researchers still work to develop an efficient method for measuring wall shear stress in blood flow, such as example, [25], [26], [27], [28]. For example, [28], proposed the Clauser plot method to estimate the shear stress of the wall in fully developed turbulent steady flow using PC and MR. The authors stated that although their method is valuable for correcting MR-based wall shear stress extraction in a fully developed steady turbulent flow, this method does not apply to *in vivo* measurements, [28].

With reference to difficulties in measuring wall shear stress in blood vessels, some researchers propose specific suspensions containing solid particles that closely approximate the flow behaviour of erythrocytes, [29], [30]. As an example, [31], studied several non-Newtonian liquids to determine how closely they simulate the flow behaviour of human blood. The authors proposed their suspension with solid particles, which approximates the flow behaviour of blood. They added an appropriate number of disc-shaped particles that stimulate red blood cells to the specific suspension. Using a laser Doppler Anemometer, the authors noted large differences in laminar velocity profiles compared to Newtonian fluids, [30]. Despite the recent achievements in the research of blood rheology, the effect of non-Newtonian blood viscosity and yield shear stress on the hydrodynamics of a blood flow, especially in transient and turbulent flow, is still not well understood.

This study deals with a bioliquid, whose physical properties are similar to human blood. Taking into account a proper rheological model together with the apparent viscosity concept, continuity, and RANS equations, and a turbulence model together with an especially developed wall damping function, simulations of transitional and turbulent flow were performed. The objective of this study is to examine the effect of high solid concentration and, as a consequence, the yield shear stress on friction in a transitional and turbulent flow of bioliquid suspension, the physical properties of which are similar to human blood. Such studies are important if mechanical or chemical methods are considered that could affect the flow rate in bioliquid.

2 Physical Model

Taking into account the results of the available studies in the literature, we can observe a similarity between the shape of erythrocytes and the solid particles in the clay kaolin suspension, [25]. Taking into account the turbulent flow of the kaolin clay suspension, one can find that the friction predictions, using the RANS equations and the apparent viscosity concept together with an

adequate rheological model, are higher compared to the measurements, [32]. The discrepancy is due to the fact that the fine dispersive solid phase modifies the viscous sublayer and the buffer layer, causing damping of the turbulence at the wall. This hypothesis was proposed by [33], [34]. Wilson and Thomas reasoned that in turbulent flow with fine solid particles, such as kaolin clay suspension, solid particles are pushed away from a wall, causing decreasing friction on a tube wall, [33], [34]. Taking into account the hypothesis of [35], [36] proposed a new damping function for the wall, including dimensionless yield shear stress. This function, together with the RANS equations and the two-equation turbulence model, successfully predicts the friction and velocity distribution in kaolin clay suspensions.

For this study, it was assumed that there exists a similarity between bioliquid suspension, similar to blood, and kaolin clay. For an argument for such an assumption, let us consider solid particles and carrier liquids of kaolin clay and blood suspensions. Comparing both suspensions, we can note that

- Solid particles in kaolin suspension:
  - solid particles are the only components suspended in water; the shape of solid particles shows similarity to the shape of erythrocytes, [30]. Solid particles are ridged.
- Solid particles in blood:
  - most solid particles in blood constitute erythrocytes; 99% of all cellular elements are erythrocytes, [4], [5]; therefore, it is assumed that erythrocytes are the only solid particles in blood; Erythrocytes are flexible.
- Carrier liquid in kaolin:
  - water is a carrier liquid for solid particles.
- Carrier liquid in blood:
  - plasma is a carrier liquid for erythrocytes; however, plasma contains approximately 90% water, [3]; therefore, it was assumed that water is a carrier liquid for erythrocytes.

It is seen above that the major difference between both suspensions is the stiffness of the solid particle since they are flexible in the case of blood and ridged in the case of kaolin suspension.

In addition to the similarity between kaolin and bioliquid, it should be noted that experiments showed that erythrocytes migrate from the wall to the centre of the blood vessel, leading to a cell-free layer at the wall of the vessel, [37], [38], as a result of which there can be a decrease in friction on the wall of the aorta. This phenomenon is similar to that in kaolin clay suspension, since Wilson and Thomas reasoned that in the case of a fine-dispersive mixture, the decrease of friction occurs on a tube wall, [33], [34]. The same conclusion with respect to blood flow was also found by [27]. The authors used several turbulence models to predict fully or partially developed turbulent flow in the aorta case and observed consistently lower values of wall shear stress from MR compared to CFD results, [27]. For this reason, the successfully validated mathematical model for kaolin clay suspension will be used to predict transitional and turbulent bioliquid flow.

In [39], measurements indicated that the mean diameters of the femoral artery in male and female subjects are approximately 9.8 mm and 8.2 mm, respectively. Therefore, for this study, a tube with a rigid wall and an inner diameter equal to 8 mm was arbitrarily chosen. The flow was assumed to be steady, homogeneous, incompressible, axially symmetric, and without circumferential swirls.

The physical model assumes that the physical properties of the bioliquid suspension are similar to those of human blood. Solid concentration is the fundamental parameter that determines the physical properties of the bioliquid. Taking into account the measurements of [40], who conducted experiments on human blood for moderate and high concentrations of erythrocytes, it was decided that two volumetric solid concentrations equal to 43% and 70% will be considered. The density of blood is approximately 1,060 kg/m^3 and depends on the concentration of erythrocytes and the temperature. Human blood density was measured by several researchers, such as, for example, [41], [42]. According to the [42], measurements, the blood density at 37°C for two volumetric concentrations of erythrocytes is stated in Table 1. The density was assumed to be constant.

The rheological model for the bioliquid suspension is a crucial point in a mathematical model. The researchers applied a macroscopic approach mainly and used the Couette viscometer to determine the dependence of the shear rate on the shear stress, [43], [44], [45], [46]. In [40], the authors used radially symmetric coaxial cylinders (Couette) and made measurements of shear stress versus shear rate for erythrocyte concentrations equal to 43% and 70% by volume. There are several rheological models recommended for human blood, like, for instance: Bingham, Ostwalda–de Waele, Carreau, Casson, or Herschel-Bulkley. The Bingham model is too simple because it includes constant viscosity. Two- and three-parameter models, such as Casson or Herschel-Bulkley, describe the dependence of the shear rate on the shear stress more accurately, [39], [40]. For this study, the Casson model was arbitrarily chosen, as some researchers recommend this model, as suitable

and simpler compared to the Herschel-Bulkley model, [40], [45], [46].

The Casson rheological model is described by Equations (1) and (2) as follows, [47]:

$$\tau^{1/2} = \tau_o^{1/2} + (\mu_\infty \gamma)^{1/2} \quad \text{for} \quad \tau > \tau_o \qquad (1)$$

and

$$\gamma = 0 \quad \text{for} \quad \tau \le \tau_o \qquad (2)$$

Equation (2), however, meets a special situation if, for some reason, the wall shear stress is below the yield shear stress. This situation will not be considered in this study.

Taking into account the concept of apparent viscosity, [48], one can write.

$$\tau = \mu_{app}\, \gamma \qquad (3)$$

Using Equations (1) and (3), the following equation can be obtained for the apparent viscosity.

$$\mu_{app} = \left[\left(\frac{\tau_o}{\gamma}\right)^{1/2} + \mu_\infty^{1/2}\right]^2 = \frac{\mu_\infty}{\left[1-\left(\frac{\tau_o}{\tau}\right)^{1/2}\right]^2} \qquad (4)$$

Finally, the apparent viscosity is calculated as follows.

$$\mu_{app} = \frac{\mu_\infty}{\left[1-\left(\frac{\tau_o}{\tau_w}\right)^{1/2}\right]^2} = \frac{\mu_\infty}{\left[1-\left(\frac{\tau_o}{\frac{dp}{dx}\frac{D}{4}}\right)^{1/2}\right]^2} \qquad (5)$$

Finally, Equation (5) was used in the mathematical model. Equation (5) has to satisfy the condition that WSS > YSS.

Based on the best match of the shear stress predictions of the Casson model with measurements performed by [40], for erythrocyte concentrations equal to 43% and 70% by volume, the following parameters of the Casson model were obtained, respectively.

$$\tau^{1/2} = 0.0325^{1/2} + (0.0039\,\gamma)^{1/2} \qquad (6)$$

$$\tau^{1/2} = 0.085^{1/2} + (0.0047\,\gamma)^{1/2} \qquad (7)$$

The rheological properties of the bioliquid are collected in Table 1.

Table 1. Rheological and physical properties of bioliquid for solid phase concentration equal to 43% and 70% by volume and temperature 37^0 C.

Particle volumetric concentration in bioliquid	Casson model		Bioliquid density
C [%]	τ_o, [Pa]	μ_∞, [Pa s]	ρ_m, [kg/m^3]
43	0.0325	0.0039	1060.00
70	0.0850	0.0047	1066.20

Figure 1a and Figure 1b present the measurements of [40], and the calculations using the Casson model, described by Equations (6) and (7) for two concentrations of erythrocytes (C=43% and C=70%). It is seen that the calculated wall shear stress and the apparent viscosity agree well with the measurements. The Casson model in the form described by Equations (6) and (7) was applied to the mathematical model of the transient and turbulent bioliquid flow.

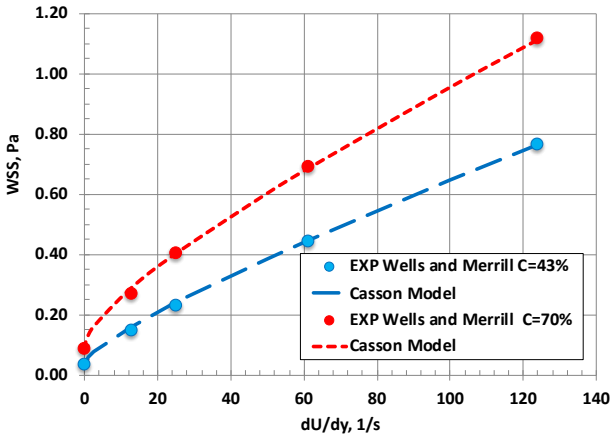

Fig. 1a: Dependence of the shear rate on the wall shear stress, [40], experimental data for human blood with C=43% and C=70%, and calculations using the Casson model described by Equations (6) and (7).

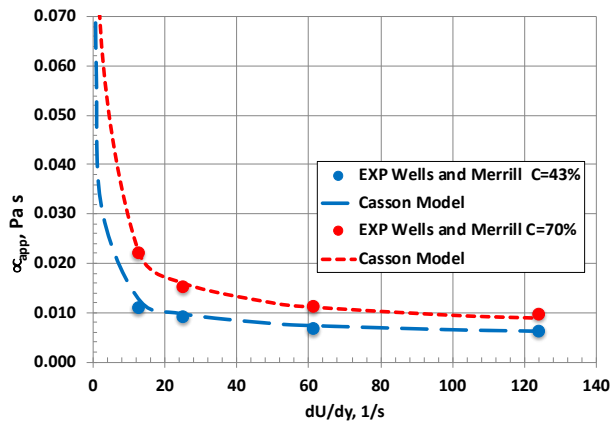

Fig. 1b: Dependence of the shear rate on apparent viscosity, [40], experimental data for human blood with C=43% and C=70%, and calculations using the Casson model described by Equations (6) and (7).

The heart of an average person, under normal conditions, beats about 72 times per minute. During every heartbeat, the ventricles pump about 70 ml of blood. This means that the heart pumps about 5 litres of blood per minute. The increase in oxygen consumption must be met primarily by an increase

in blood flow, which can even increase five times during exercise, [49]. For such an extreme flow rate, it is reasonable to consider transitional and even turbulent flow, [50]. However, it was arbitrarily assumed that the maximum Reynolds number cannot exceed 5,000.

3 Mathematical Model

The mathematical model constitutes continuity and randomly averaged Navier-Stokes equations (RANS). As the flow is axially symmetrical, the cylindrical coordinates (x, r, θ) were applied. In this case, the *ox* coordinate lies on the symmetry axis of the aorta, while the *or* coordinate is the radial distance from the symmetry axis. According to the assumption that the bioliquid flow is axially symmetric and without circumferential swirls, the velocity components V and W are equal to zero.

Taking into account the assumption stated in the physical model, the continuity equation can be described as follows.

$$\frac{\partial}{\partial x}(\bar{\rho}_m \bar{U}) = 0 \tag{8}$$

Equation (8) indicates that the flow is fully developed, which means that the velocity distribution $\bar{U}$ in the *ox* direction does not change because the density is constant. Therefore, including Equation (9) in the time-averaged Navier-Stokes equations, we can write the final form in cylindrical coordinates as follows.

$$\frac{1}{r}\frac{\partial}{\partial r}\left[r\left(\mu_{app}\frac{\partial \bar{U}}{\partial r} - \bar{\rho}_m \overline{u'v'}\right)\right] = \frac{\partial \bar{p}}{\partial x} \tag{9}$$

The dashed lines in the continuity and momentum equations represent the time-averaged quantities. The apparent viscosity in Equation (9) is calculated using Equation (5), while the component of the turbulent stress tensor is designated taking into account the Boussinesque hypothesis, [51], which is an indirect method and describes the turbulence using turbulent viscosity (μ_t), which is a scalar quantity. The component of the turbulent stress tensor in Equation (9) was expressed as follows.

$$-\bar{\rho}_m \overline{u'v'} = \mu_t \frac{\partial \bar{U}}{\partial r} \tag{10}$$

In [52], [53], the authors successfully examined several k-ε models for low Reynolds numbers for homogeneous and pseudo-homogeneous suspensions. Studies have shown that the Launder and Sharma k-ε turbulence model for low Reynolds numbers is one of the first and most widely used models and has been shown to agree well with experimental and DNS data for a wide range of turbulent flow problems, performing better than other k–ε models, [54], [55], [56], [57]. In addition to that, the model has great potential to predict non-Newtonian flows, [58]. Therefore, in [59], a turbulence model was chosen to calculate the component of the turbulent stress tensor. Launder and Sharma performed dimensional analyses with the assumption that turbulent viscosity (μ_t) depends on the kinetic energy of turbulence (k) and its dissipation rate (ε), and the density of the fluid (ρ). In [59], the authors proposed the following expression for turbulent viscosity.

$$\mu_t = f_\mu \frac{\bar{\rho}_m}{\varepsilon} k^2 \tag{11}$$

The function f_μ in Equation (11) is called the *turbulence damping function* or the *wall damping function* and causes a reduction in turbulent viscosity if a distance from the wall of a tube approaches zero. This function was developed empirically by matching predictions with measurements, [59]. The function is as follows.

$$f_\mu = 0.09\, exp\left[\frac{-3.4}{\left(1+\frac{Re_t}{50}\right)^2}\right] \tag{12}$$

The turbulent Reynolds number (Re_t) in Equation (12) was developed from a dimensionless analysis, [59], as follows.

$$Re_t = \frac{\rho_m k^2}{\mu_{app}\,\varepsilon} \tag{13}$$

The equations for the kinetic energy of turbulence and its dissipation rate were derived from the Navier-Stokes equations using a time-averaged procedure, [59], [60]. Taking into account the assumptions made in the physical model, the final form of both equations is as follows.

$$\frac{1}{r}\frac{\partial}{\partial r}\left[r\left(\mu_{app}+\frac{\mu_t}{\sigma_k}\right)\frac{\partial k}{\partial r}\right] + \mu_t\left(\frac{\partial \bar{U}}{\partial r}\right)^2 = \bar{\rho}_m \varepsilon + 2\mu_{app}\left(\frac{\partial k^{1/2}}{\partial r}\right) \tag{14}$$

$$\frac{1}{r}\frac{\partial}{\partial r}\left[r\left(\mu_{app}+\frac{\mu_t}{\sigma_\varepsilon}\right)\frac{\partial \varepsilon}{\partial r}\right] + C_1\frac{\varepsilon}{k}\mu_t\left(\frac{\partial \bar{U}}{\partial r}\right)^2 = C_2[1 - 0.3\, exp(-Re_t^2)]\frac{\bar{\rho}_m \varepsilon^2}{k} - 2\frac{\mu_{app}}{\bar{\rho}_m}\mu_t\left(\frac{\partial^2 \bar{U}}{\partial r^2}\right) \tag{15}$$

It must be emphasised that taking into account the mathematical model in the form presented above to simulate suspension flow such as kaolin clay, the predicted friction is higher than the measurements. As noted above, the Wilson and Thomas hypothesis indicates that for such suspensions the fine solid particles modify the viscous sublayer and the buffer layer, causing the particles to pull away from the wall of the tube toward the symmetry axis, [33],

[34]. Several researchers reached a similar conclusion on blood flow, [27], [37], [38]. In [27], authors used several turbulence models to predict fully or partially developed turbulent flow in an aorta case and observed consistently lower values of wall shear stress from MR compared to CFD results. For this reason, Equation (12), which describes the wall damping function, was replaced by Equation (16), proposed by [35], [36].

$$f_\mu = 0.09\ exp\left[\frac{-3.4\left(1+\frac{\tau_o}{\tau_w}\right)}{\left(1+\frac{Re_t}{50}\right)^2}\right] = 0.09\ \mathrm{EXP}\left[\frac{-3.4\left(1+\frac{\tau_o}{\frac{dp}{dx}\frac{D}{4}}\right)}{\left(1+\frac{Re_t}{50}\right)^2}\right] \quad (16)$$

The wall damping function (16) depends on the yield and wall shear stresses and, together with the above mathematical model, was validated for several suspensions in a wide range of solid concentrations, yield stresses, tube diameters, and Reynolds number, and provided fairly good predictions of friction and velocity profiles, [35], [36], [52], [53]. This function is important at a close distance from a tube wall and its importance is negligible in the core region. If the ratio of the yield stress to the wall shear stress is zero, the damping function (16) approaches the standard function defined by Equation (12).

Finally, the mathematical model constitutes partial differential Equations (9), (14), (15) and complementary relations (8)-(11), (13), and (16). Taking into account the bioliquid properties, stated in Table 1, simulations of transitional and turbulent flow were performed. The constants presented in Equations (14) and (15) are the same as those proposed by Launder and Sharma and are the following: C_1=1.44; C_2=1.92; σ_k=1.0; σ_ε=1.3, [59].

4 Numerical Computations

The mathematical model is dedicated to the transitional and turbulent flow of suspension, similar to blood, which exhibits non-Newtonian characteristics of the yield shear stresses. The set of equations has four dependent variables, namely, the velocity component U(r), the static pressure p(x), the kinetic energy of the turbulence k(r), and its dissipation rate ε(r). However, we have only three partial differential equations, namely (9), (14), and (15). For this reason, computations are performed for *a priori* known ∂p/∂x. In such an approach, the dependent variables are U(r), k(r), and ε(r). For known ∂p/∂x the equation set is closed, that is, the number of dependent variables is equal to the number of partial differential equations. For the assumed value of ∂p/∂x, computations of U(r), k(r), and ε(r) are performed based on which the Reynolds number is calculated. If the Reynolds number is beyond the assumed range the new value of ∂p/∂x is used until reaching the estimated range of Re.

The following boundary conditions were applied to the mathematical model.

- for the wall of the aorta, r=R:

$$U=0,\ k=0 \text{ and } \varepsilon=0; \quad (17)$$

- for the aorta symmetry axis, r=0:

$$\partial U/\partial r=0,\ \partial k/\partial r=0,\ \partial \varepsilon/\partial r=0; \quad (18)$$

which means that for r=R there is no sleep for the dependent variables, while on the symmetry axis (r=0) axially symmetric conditions were applied to all the dependent variables.

The set of differential equations was computed using the final volume method, with an iteration procedure, [61], and its computer code. The calculations were carried out for 80 nodal points not uniformly distributed in the radius of the tube. Most of the nodal points were located in the vicinity of a tube wall to ensure the convergence process. The number of nodal points was set experimentally to ensure nodally independent computations. The iteration cycles were repeated until a convergence criterion, defined by Equation (19), was achieved.

$$\sum_j \left|\frac{\emptyset_j^n - \emptyset_j^{n-1}}{\emptyset_j^n}\right| \le 0.0005 \quad (19)$$

where $\emptyset_j^n$ is the general dependent variable that ∅=U, k, ε, and 'j' is the nodal point, and 'n' is the iteration cycle, while $\emptyset_j^{n-1}$ is the nodal point 'j' after the (n-1) iteration cycle.

5 Results of the Simulations

Numerical simulations were performed using the mathematical model described by Equations (5), (8)-(11), (13)-(16) for two sets of bioliquid concentrations equal to 43% and 70% by volume and rigid horizontal tube with inner diameter D=8 mm. The rheological and physical properties of the bioliquid suspension are presented in Table 1. Because the bioliquid yield shear stress is relatively low, it was assumed that the Reynolds number is the same as that for Newtonian liquids and is described as follows.

$$\mathrm{Re} = \frac{\bar{\rho}_m\, U_b\, D}{\mu_{app}} \quad (20)$$

Assuming that there is a transitional flow for 2,300<Re<4,000, and a turbulent one for Re>4,000, the numerical simulations were performed for Reynolds numbers in the range of 2,615 to 5,000. The maximum Reynolds number equal to Re =

5,000 was arbitrarily chosen as sufficiently high for humans under intensive exercises.

Taking into account Equation (5) one can calculate the dependence of WSS on the apparent viscosity of the bioliquid suspension for two solid concentrations equal to 43% and 70%; see Figure 2a. It is obvious that the apparent viscosity decreases as the WSS increases. However, the decrease rate depends on the solid concentration and is higher for C=70% than for C=43%. The relative difference in apparent viscosities is higher by ab. 25% for C=70% compared to C=43%.

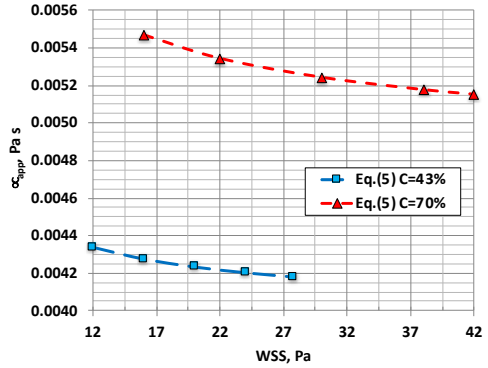

Fig. 2a: Dependence of wall shear stress on apparent viscosity – Eq. (5); Simulations of apparent viscosity for bioliquid suspensions for C=43% and C=70%.

Analysing Figure 2a one can see that for bioliquid suspension with C=43%, the WSS is in the range from 12 to 27.8 [Pa], while for C=70% it is 16 to 42. This is because in both cases the Reynolds number is in the range from Re=2,615 to Re=5,000. To illustrate this, Figure 2b shows the same results as Figure 2a, but refers to the Reynolds number. In this case, predictions were made using a mathematical model for transitional and turbulent flow.

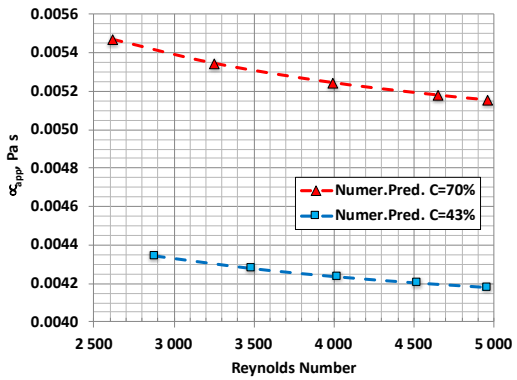

Fig. 2b: Dependence of Reynolds' number on apparent viscosity – numerical predictions; Simulations of apparent viscosity for bioliquid suspensions for C=43% and C=70%.

Analysing Figures 2a and 2b, one can see that for bioliquid with C=43% the first point has coordinates (Re=2,885; WSS=12 [Pa]) and the last one (Re=4,961, WSS=27.8 [Pa]) while for C=70% it is (Re=2,615, WSS=16 [Pa]) and (Re=4,964, WSS=42 [Pa]), respectively.

From the balance of forces acting on the suspension that flows in a horizontal tube with a constant inner diameter D and length L, we can get the following.

$$\frac{\Delta p}{L} = \frac{4\,\tau_w}{D} \tag{21}$$

The term Δp/L in Equation (21) represents the term $\partial p/\partial x$ in the momentum Equation (9) and it is named the *pressure gradient* or the *frictional head loss* and shows the energy losses in a flowing suspension. Equation (21) shows that for constant tube diameter, the frictional head loss (Δp/L) and the wall shear stress (τ_w) are qualitatively the same. Blood flow plays an important role in oxygen transport and is highly dependent on friction. Higher friction causes a lower flow rate for the same pressure generated by the pump (heart). Therefore, decreasing frictional head loss in flowing blood is a great challenge of fluid mechanics and biomechanics. In reference to the reduction of blood friction, we recognise two main approaches. The first one is the mechanical approach, which mainly deals with increasing vessel diameter, i.e. by inserting a stent with a higher inner diameter compared to a natural vessel. The second approach uses chemical additives in order to decree blood viscosity and as a consequence increase the flow rate.

To see the effect of the concentration of solid particles in bioliquid suspension on wall shear stress (WSS), proper simulations were performed for C=43% and C=70%. Figure 3 shows the results of the predicted WSS versus the flow rate for bioliquid suspension similar to blood with C=43% and C=70% and for water at a constant temperature equal to 20 °C. It is seen that the data for water are much lower than those for bioliquid.

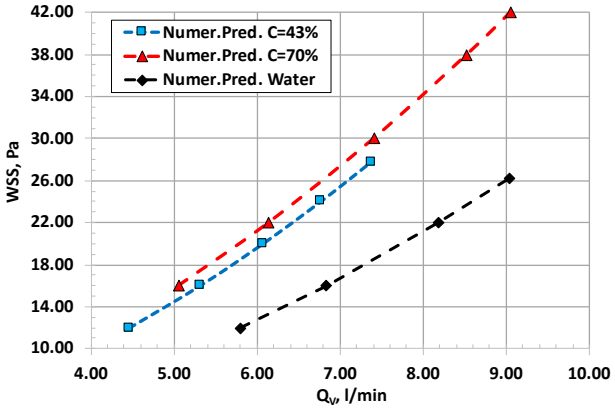

Fig. 3: Simulations of the dependence of flow rate on WSS for bioliquid suspension similar to blood for C=43% and C=70%, and for water.

The numerical simulations presented in Figure 3 demonstrate that suspension with C=70% (τ_o=0.085 [Pa]) exhibits higher wall shear stress compared to C=43% (τ_o=0.0325 [Pa]) which is not surprising. Average relative differences are about 10% and 6% in the transitional (2,300<Re<4,000) and turbulent-flow regimes (Re>4,000), respectively. Assuming that there is a fully turbulent suspension flow for Re>4,000, it was calculated that for suspension with C=70% the WSS=30 [Pa] for Re=4,000, while for C=43% the WSS=26 [Pa].

The friction factor simulations for two different solid concentrations (two different yield stresses) in the suspension flow rate range of 5 to 9 [l/min] are presented in Figure 4a. The results show that for a constant flow rate, the friction factor is significantly higher for C=70% than for C=43%. The average relative difference is about 7% and depends on the flow rate. Simulations of the friction factor λ in the Reynolds number range of 2,615 to 5,000 are presented in Figure 4b. In Figure 4b, it is seen that the friction factor λ is the same for both solid concentrations. This is consistent with an earlier assumption that because the YSS is relatively low, the Reynolds number can be the same as that for a Newtonian liquid.

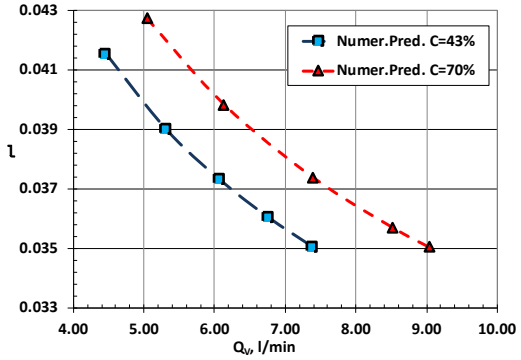

Fig. 4a: Dependence of bioliquid flow rate on friction factor; Simulations of friction factor in bioliquid suspension for C=43% and C=70%.

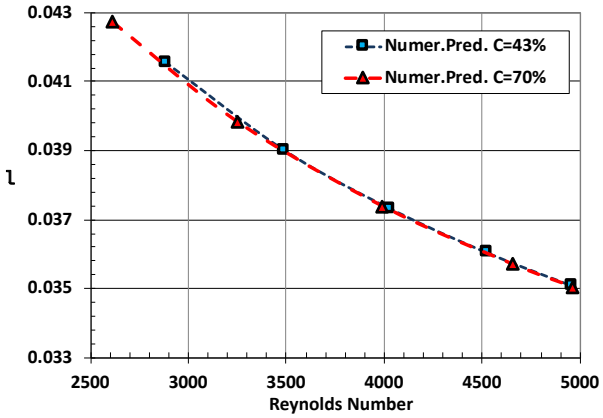

Fig. 4b: Dependence of Reynolds' number on friction factor; Simulations of friction factor in bioliquid suspension for C=43% and C=70%.

6 Discussion

Experiments with *in vivo* blood flow are extremely difficult. Difficulties arise with the decrease in the dimension of the flow domain even when new technologies are applied, [62]. The exact position of the flow domain (vessel) is not known beforehand because it is moving when the pump (heart) is working. Even a small error in boundary identification significantly influences the measurements. For this reason, we still face difficulties in accessing reliable measurements of blood friction. Such measurements are essential for the validation of mathematical models.

It was mentioned in the physical model that some researchers observed a similarity between the shape of erythrocytes and the clay kaolin particles, [30]. Erythrocytes and kaolin particles have similar sizes and shapes and tend to form rouleaux at a low shear rate, causing an increase in yield shear stress and viscosity, [20], [21]. Another similarity is associated with the tendency of solid particles to migrate from the wall to the centre of the blood vessel, leading to

a cell-free layer on the wall of the vessel, [27], [37], [38], as a result, a decrease in friction can appear on the wall of the tube, [63]. This phenomenon was also observed by [33], [34], in the case of kaolin clay suspension. For this reason, the mathematical model, which was well examined for the suspension of kaolin, has been used in this study to predict the bioliquid flow.

In the literature, no predictions for transitional or turbulent blood flow with a high concentration of erythrocytes, like 70%, were found, including the concept of damping of turbulence. This study presents the results of simulations of suspensions similar to those of blood, assuming an analogy between kaolin clay and blood suspensions. Of course, there are also some differences since erythrocytes are deformable, whereas solid particles of kaolin clay are not. The aorta and other vessels are flexible, whereas industrial transport of kaolin clay exists in rigid pipelines. Despite these differences, it is valuable to examine the influence of the high solid concentration and as a consequence the yield shear stress, on energy losses in a transitional, and turbulent flow of the suspension similar to blood in a narrow tube.

The crucial point in this study is the range of flow rates and the range of Reynolds numbers. It is known that in some circumstances, such as physical activity, the flow of human blood in an aorta could be transitional or turbulent. In the analysis of turbulent flow, it was assumed that the Reynolds number does not exceed 5,000. The reason for such an assumption comes from the research of [49], [50]. The authors noted that increased oxygen consumption must be met primarily by increased blood flow, which can increase even five times during exercise. This means that we could expect that in some circumstances the blood flow rate may exceed 25 [l/min], as the typical human blood flow rate is approximately 5 [l/min], [49]. In this study, the flow rate was arbitrarily chosen in the range between 5 and 9 [l/min], which seems reasonable.

The studies of blood flow available in the literature deal with the concentration of erythrocytes below 45%, [12], [43], [64]. However, if the concentration of erythrocytes increases, which is due to physical activity or disease, the shear stress of the product also increases. When analysing Equation (5), it is seen that an increase in the yield shear stress results in an increase in apparent viscosity. To analyse this, Equation (5) will be used to calculate the apparent viscosity for an arbitrarily chosen range of YSS, that is, from τ_0=0 to τ_0=0.10 [Pa], and for solid concentration C=70%, and WSS equal to τ_w=5, τ_w=15 and τ_w=60 [Pa]. The range of WSS from 5 to 60 [Pa] was intentionally chosen according to laminar, transitional, and turbulent flow, respectively. The results of the calculations are presented in Figure 5a. When analysing Figure 5a, it can be concluded that the apparent viscosity increases as YSS increases. Therefore, for the same density of suspension, tube diameter, and YSS, the apparent viscosity in laminar flow is higher than in transitional or turbulent flow. Additionally, a lower value of WSS results in a higher influence of YSS on apparent viscosity; see Figure 5a. Finally, it can be concluded that the importance of the yield shear stress decreases with increasing Reynolds number. This is even more pronounced if we take into account the fact that, in the case of transitional and turbulent flow, the importance of apparent viscosity has a secondary meaning, since turbulent viscosity tends to dominate.

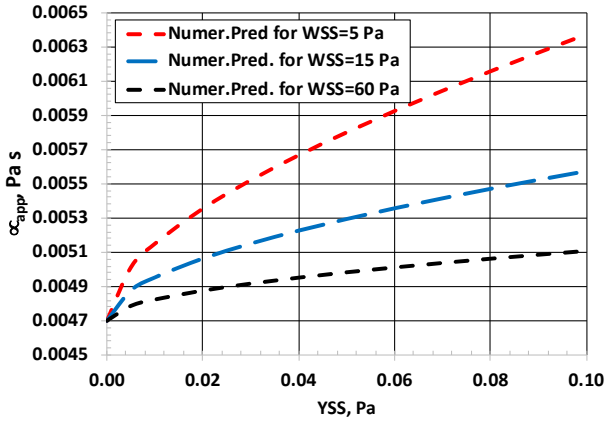

Fig. 5a: Dependence of YSS on apparent viscosity for the WSS chosen; Importance of YSS in bioliquid suspension for constant D=0.008m, and C=70%.

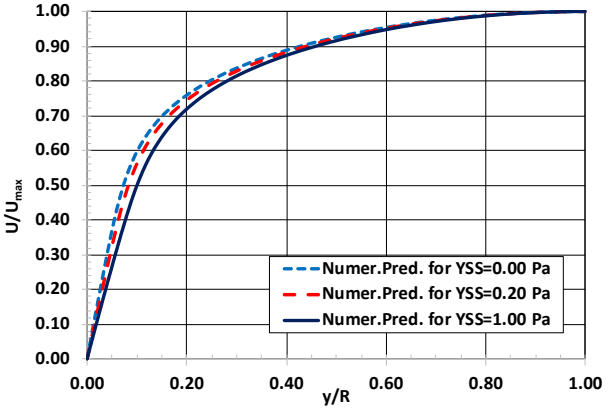

Fig. 5b: Dimensionless velocity profiles of bioliquid suspensions for the chosen YSS and constant flow rate Q_v=7.5 [l/min]; Importance of YSS in bioliquid suspension for constant D=0.008 [m], and C=70%.

Figure 5b presents the influence of the chosen YSS on dimensionless velocity profiles in the turbulent flow of the bioliquid suspension for a

constant flow rate equal to 7.5 [l/min] and for a constant tube diameter D=8 mm, solid concentration C = 70% and viscosity μ_∞=0.0047 [Pa s]. It is seen that with an increase in YSS, the velocity profiles change significantly. If the YSS increases the velocity profiles have a clear tendency to change shape from flat to parabolical one - see Figure 5b. It is worth highlighting that the influence of damping of turbulence, expressed by Equation (16), on the frictional loss and velocity profile is not substantial because the YSS compared to the WSS is relatively small and its importance decreases with increasing Reynolds number.

7 Conclusions

Human blood flow is extremely complex, and there is no universal model for its predictions. Based on simulation made for bioliquid suspensions similar to blood in transitional or turbulent flow with moderate and high solid concentrations, using the apparent viscosity concept, Casson rheological model, and turbulence model for low Reynolds numbers, and the wall damping function, the following conclusions can be formulated.

1. The Casson model is suitable to predict bioliquid rheology for moderate (C=43%) and high solid concentrations (C=70%); see Figure 1a and Figure 1b.
2. If the solid phase concentration increases, the yield shear stress, the apparent viscosity, and the wall shear stress also increase; see Figure 1a, Figure 1b, Figure 2a, Figure 2b, and Figure 3.
3. The increase in solid concentration from C=43% (τ_o=0.0325 [Pa]) to C=70% (τ_o=0.085 [Pa]), causes an increase in wall shear stress of approximately 10% and 6% for transitional and turbulent flow, respectively, while compared to water, the differences are substantial; see Figure 3.
4. The influence of the yield shear stress (or solid concentration) on energy losses cannot be neglected if a transitional or turbulent flow of the bioliquid suspension is considered; see Figure 3 and Figure 4a. However, the importance of the yield shear stress decreases with increasing Reynolds number; see Figure 5a.
5. For the same flow rate, the friction factor of the bioliquid suspension with C=70% is higher than for C=43% and the average relative difference is approximately 8%.
6. Changes in the yield shear stress result in changes in the shape of the velocity distribution. If the YSS increases, the velocity profiles have a clear tendency to change shape from flat to parabolic; see Figure 5b.
7. The influence of turbulence damping, expressed by Equation (16), on frictional loss and the velocity profile is not substantial because the YSS compared to the WSS is relatively small and its importance decreases with increasing Reynolds number.

The paper contributes to the discussion between scientists as to whether the rheological properties of blood are important or not in the prediction of the shear stress of the blood wall or the velocity profiles.

When the results of bioliquid flow simulations are taken into account, it is permissible to conclude that the frictional losses increase with increasing solid concentration or YSS. The inclusion of a proper rheological model to predict laminar bioliquid flow is essential, while for transitional and turbulent flow it is less important, as the increase in wall shear stress for the parameters studied was approximately 10% and 6%, respectively.

Future studies are needed to better understand the flowing nature of bioliquid, which is similar to that of blood; especially, attention is needed on the process of particle migration from the tube wall to the symmetry axis and its effect on WSS. However, this requires reliable measurements on a vessel wall.

Other future studies should focus on a better understanding of the bioliquid flow near the vessel wall during the acceleration and deceleration phases. Also, the influence of temperature on the rheological properties of bioliquid and flow structure is very desired.

Nomenclature

C – concentration of solid particles by volume, %
C_i –constants in the Launder and Sharma turbulence model, i=1, 2
f_μ – turbulence damping function at the tube wall
k – kinetic energy of turbulence, m^2/s^2
L – tube length, m
p – static pressure, Pa
Q_v – flow rate, l/min
r – radial distance from symmetry axis / axial coordinate, m
R – inner tube radius, m
Re – Reynolds number
u', v' – fluctuating components of suspension velocity in ox and or directions, m/s
U – suspension velocity component in x direction, m/s
V – suspension velocity component in r direction, m/s

W – suspension velocity component in θ direction, m/s
WSS – wall shear stress, Pa
x – axial coordinate, m
y – distance from the tube wall, m
YSS – yield shear stress, Pa

Greek symbols

γ – share rate; shear deformation, strain rate, s^{-1}
ε – rate of dissipation of kinetic energy of turbulence, m^2/s^3
θ – angle around the symmetry axis of the tube / tangential coordinate, deg
λ – friction factor
μ_∞ – suspension viscosity, Pa s
ρ – suspension density, kg/m^3
σ_k – effective Prandtl-Schmidt number for k
σ_ε – effective Prandtl-Schmidt number for ε
τ, τ_0 – shear stress / yield shear stress, Pa
Φ – general dependent variable, Φ=U, k, ε

Subscripts:

app – apparent viscosity
b – bulk (cross section average value)
t – turbulent

References:

[1] Shook, C.A. and Roco, M.C., Slurry Flow: Principles and Practice, Ed. Brenner, H., Butterworth-Heinemann, Boston, **2015**, p. 324.

[2] Dohnalova, Z., Svoboda, L., Šu cová, P., Characterization of kaolin dispersion using acoustic and electroacoustic spectroscopy. *Journal of Mining and Metallurgy*, **2008**, 44 B, pp. 63-72.

[3] Alexander, D.E., Nature's Machines. An Introduction to organismal biomechanics, *Academic Press. Elsevier*, **2017**, p. 425.

[4] Earl, E. and Mohammadi, H., Biomechanics of Human Blood, **2018**.

[5] Tomschi, F., Bizjak, D., Bloch, W., Latsch, J., Predel, H. G., Grau, M., Deformability of different red blood cell populations and viscosity of differently trained young men in response to intensive and moderate running, *Clin. Hemorheol. Microcirc.*, **2018**, vol. 69, pp. 503–514.

[6] Lapoumeroulie, C., Connes, P., El Hoss, S., Hierso, R., Charlot, K., Lemonne, N., New insights into red cell rheology and adhesion in patients with sickle cell anaemia during vaso-occlusive crises, *Br. J. Haematol.*, **2019**, vol. 185, pp. 991–994.

[7] Ellsworth, M.L., The red blood cell as an oxygen sensor: what is the evidence? *Acta Physiol. Scand.*, **2000**, vol.168, pp.551–559.

[8] Lanotte, L., Mauer, J., Mendez, S., Fedosov, D. A., Fromental, J. M., Claveria, V., Red cells' dynamic morphologies govern blood shear thinning under microcirculatory flow conditions, *Proc. Natl. Acad. Sci. USA.*, **2016**, vol.113, pp.13289–13294.

[9] Ugurel, E., Piskin, S., Aksu, A.C., Eser, A., Yalcin, O., From experiments to simulation: shear-induced responses of red blood cells to different oxygen saturation levels, *Frontiers in Physiology*, **2019**, vol. 10, 1559.

[10] Pop, G. A., Duncker, D. J., Gardien, M., Vranckx, P., Versluis, S., Hasan, D., The clinical significance of whole blood viscosity in cardio-vascular medicine, *Neth. Heart J.* **2002**, vol. 10, No.12, pp.512–516. PMC2499821.

[11] Formaggia, L., Lamponi, D., Quarteroni, A., One-dimensional models for blood flow in arteries. *J. Engineering Mathematics*, **2003**, vol. 47, pp.251-276.

[12] Shipkowitz, T., Rodgers V.G., Frazin L.J., Chandran K.B., Numerical study on the effect of secondary flow in the human aorta on local shear stresses in abdominal aortic branches, J. *Biomech.*, **2000**, vol.33 No. 6, pp. 717-728.

[13] Miyazaki, S., Itatani, K., Furusawa, T., Nishino, T., Validation of numerical simulation methods in aortic arch using 4D flow MRI, *Heart and Vessels*. **2017**, vol. 32, No.8, pp.1032–44.

[14] Xu, D., Warnecke, S., Song, B., Transition to turbulence in pulsating pipe flow, *J. of Fluid Mechanic*, **2017**, vol. 831, pp. 418–32.

[15] Xu, D. and Avila, M., The effect of pulsation frequency on transition in pulsatile pipe flow, *J. of Fluid Mechanics*, **2018**, vol. 857, pp. 937–51.

[16] Alasakani, K., Tantravahi, R.S.I., Kumar P.T.V., On refining the input data set to mathematical models simulating arterial blood flow in humans, WSEAS Transactions on Fluid Mechanics, **2021**, vol. 16, pp.63-78.

[17] Nader, E., Skinner, S., Romana, M., Fort, R., Lemonne, N., Guillot, N., Gauthier, A., Antoine-Jonville, S., Renoux, C., Hardy-Dessources, M.D., Stauffer, E., Joly, P., Bertrand, Y., Connes, P., Blood rheology: Key parameters, Impact on blood flow, Role in sickle cell disease and effects of exercise, *Front Physiol.*, **2019**, vol. 10, pp.1-14.

[18] Lemonne, N., Connes, P., Romana, M., Vent-Schmidt, J., Bourhis, V., Lamarre, Y., Increased blood viscosity and red blood cell aggregation in a patient with sickle cell anemia and smoldering myeloma, *Am. J. Hematol*., **2012**, vol.87, E129.

[19] Vandewalle, H., Lacombe, C., Lelièvre, J. C., Poirot, J.C., Blood viscosity after a 1-h submaximal exercise with and without drinking. *Int. J. Sports Med*., **1988**, vol.09, No.2, pp.104-107.

[20] Abbasi, M., Farutin, A., Ez-Zahraouy, H., Benyoussef, A., Misbah, C., Erythrocyte - erythrocyte aggregation dynamics under shear flow. *Physical Review Fluids*, **2021**, vol. 6, 023602.

[21] Wu, Y., Hsu, P., Tsai, C., Pan, P., Chen, Y., Significantly increased low shear rate viscosity, blood elastic modulus, and RBC aggregation in adults following cardiac surgery. *Scientific Reports*, **2018**, vol. 8, No. 7173, pp. 1–10.

[22] Lee, CA. and Paeng, DG., Numerical simulation of spatiotemporal red blood cell aggregation under sinusoidal pulsatile flow. *Scientific Reports*, **2021**, vol. 11, No. 9977.

[23] Thomas, D.G., Turbulent disruption of flocs in small particle size suspensions. *AIChE J*., **1964**, vol. 10. No. 4, pp. 517-523.

[24] Michaels, A.S. and Bolger, J.C., The plastic flow behavior flocculated kaolin suspensions, *Industrial & Engineering Chemistry Fundamentals*, **1962**. Vol. 1, No. 3, pp. 153-162.

[25] Zimmermann, J., Demedts, D., Mirzaee, H., Ewert, P., Stern, H., Meierhofe, C., Menze, B., Henne, A., Wall shear stress estimation in the aorta: Impact of wall motion, spatiotemporal resolution, and phase noise, *J. Magn. Reson. Imaging*, **2018**, 48, pp. 718-728.

[26] Masutani, E.M., Contijoch, F., Kyubwa, E., Cheng, J., Alley, M.T., Vasanawala, S., Hsiao, A., Volumetric segmentation-free method for rapid visualization of vascular wall shear stress using 4D flow MRI, *Magn. Res. Med*., **2018**, 80(2), pp. 748-755.

[27] Szajer, J. and Ho-Shon, K., A comparison of 4D flow MRI-derived wall shear stress with computational fluid dynamics methods for intracranial aneurysms and carotid bifurcations — A review, *Magnetic Resonance Imaging,* **2018**, 48, pp. 62-69.

[28] Shokina, N., Bauer, A., Teschner, G., Buchenberg, W.B., Tropea, C., Egger, H., Hennig, J., Krafft, A.J., MR-based wall shear stress measurements in fully developed turbulent flow using the Clauser plot method. *J. Magn. Reson*., **2019**, 305, pp. 16-21

[29] Chandra, K., Dalai, I.S., Tatsumi, K., Muralidhar, K., Numerical simulation of blood flow modeled as a fluid- particulate mixture. *Journal of Non-Newtonian Fluid Mechanics*, **2020**, vol.285, No. 104383, pp.1-8,

[30] Yahaya, S., Jikan, S.S., Badarulzaman, N.A., Adamu, A.D., Chemical composition and particle size analysis of kaolin, *Int. Electronic Scientific Journal*, **2017**, vol. 3, No. 10, pp. 1001-1004.

[31] Liepsch, D.W., Thurston, G., Lee, M., Studies of fluids simulating blood-like rheological properties and applications in models of arterial branches. *Biorheology*, **1991**, vol. 28 No. 1-2, pp. 39-52.

[32] Bartosik, A., Modelling of a turbulent flow using the Herschel-Bulkley rheological model. *Chemical and Process Engineering*, **2006**, vol. 27, pp. 623-632.

[33] Wilson, K.C. and Thomas, D.G., A new analysis of the turbulent flow of non-Newtonian fluids. *Can. J. Chem. Eng.*, **1985**, vol. 63, pp. 539-546.

[34] Thomas, D.G. and Wilson, K.C., New analysis of non-Newtonian turbulent flow—yield-power-law fluids, *Can. J. Chem. Eng*., **1987**, vol. 65, No. 2, pp. 335-338.

[35] Bartosik, A., Simulation and Experiments of Axially-Symmetrical Flow of Fine- and Coarse-Dispersive Slurry in Delivery Pipelines; *Monograph M-11*; Kielce University of Technology: Kielce, Poland, **2009**.

[36] Bartosik, A., Application of rheological models in prediction of turbulent slurry flow, *Flow, Turbulence and Combustion*, **2010**, vol. 84, No. 2, pp. 277-293.

[37] Wagner, C., Steffen, P., Svetina, S., Aggregation of red blood cells: From rouleaux to clot formation, *Comptes Rendus Physique*, **2013**, vol. 16, No. 6, pp. 459-469.

[38] Baskurt O.K. and Meiselman, H.J., Erythrocyte aggregation: basic aspects and clinical importance. *Clinical Hemorheology and Microcirculation.* **2013**; vol.53, No. 1-2, pp. 23-37 PMID: 22975932,

[39] Sandgren, T., Sonesson, B., Ahlgren, A.R., Lanne, T., The diameter of the common

femoral artery in healthy human: Influence of sex, age, and body, *J. Vascular Surgery*, **1999**, vol.29, No. 3, pp. 503-510.

[40] Wells, R.E. and Merrill, E.W., Influence of flow properties of blood upon viscosity - Hematocrit relationship, *J. Clinic Investigation*, **1962**, vol.41, No.8, pp.1591-1598.

[41] Kenner, T., The measurement of blood density and its meaning, *Basic Research in Cardiology*, **1989**, vol.84, No. 2, pp.111-124.

[42] Burstain, J.M., Brecher, M.E., Halling, V.W., Pineda, A.A., Blood volume determination as a function of Hematocrit and mass in three preservative solutions and Saline, *A.J.C.P. Coagulation and Transfusion Medicine*, **1994**, vol.102, No. 6, pp.812-815.

[43] Shibeshi, S.S. and Collins, W.E., The rheology of blood flow in a branched arterial system, *Applied Rheology*, **2005**, vol. 15, No. 6, pp. 398-505.

[44] Lee, B.K., Xue S., Nam J., Lim H., Shin S., Determination of the blood viscosity and yield stress with a pressure-scanning capillary hemorheometer using constitutive models, *Korea-Australia Rheology J.* **2011**, vol. 23, No. 1, pp. 1-6.

[45] Ruef, P., Gehm, J., Gehm, L., Felbinger, C., Pöschl, J., Kuss, N., The new low shear viscosimeter LS300 for determination of viscosities of Newtonian and non-Newtonian fluids, *General Physiology and Biophysics*, **2014**, vol.33, No. 3, pp.281-284.

[46] Ruef, P., Gehm, J., Gehm, L., Felbinger, C., Pöschl, J., Kuss, N., Determination of whole blood and plasma viscosity by means of flow curve analysis, *General Physiology and Biophysics*, **2014**, vol. 33, No.3, pp.285-293.

[47] Casson, N., A flow equation for pigment-oil suspensions of the printing ink type rheology of dispersed systems. *London Pergamon Press*, **1959**, pp. 84-104.

[48] Metzner, A.B. and Reed, J., Flow of non-Newtonian fluids - correlation of the laminar, transition and turbulent flow regions, *AIChEJ.* **1955**, pp.434-440.

[49] Ramanathan, T. and Skinner, H., Coronary blood flow, *Continuing Education in Anaesthesia Vritical Care & Pain*, **2005**, vol.5, No. 2, pp.61-64.

[50] Saqr, K.M., Tupin, S., Rashad, S., Physiologic blood flow is turbulent. Nature, *Scientific Reports*, **2020**, vol. 10, No. 15492.

[51] Boussinesque, J., Theorie de l'ecoulement tourbillant, *Mem. Acad. Sci*., **1897**, vol. 23 46.

[52] Cotas, C., Silva, R., Garcia, F., Faia, P., Asendrych D., Rasteiro, M.G., Application of different low-Reynolds k-ε turbulence models to model the flow of concentrated pulp suspensions in pipes, *Procedia Engineering*, **2015**, No. 102, pp. 1326-1335.

[53] Cotas, C., Asendrych, D., Garcia, F., Faia, P., Rasteiro, M.G., Turbulent flow of concentrated pulp suspensions in a pipe – numerical study based on a pseudo-homogeneous approach. *COST Action FP1005 Final Conference, EUROMECH Colloquium 566*, Trondheim, Norway, **2015**, pp. 31-33.

[54] Mathur, S. and He, S., Performance and implementation of the Launder–Sharma low-Reynolds number turbulence model. *Comput. Fluids*, **2013**, vol.*79*, pp. 134–139.

[55] Abir, I.A. and Emin, A.M., A comparative study of four low-Reynolds-number k-e turbulence models for periodic fully developed duct flow and heat transfer. *Numer. Heat Transf. Part B Fundam*. **2016**, vol. *69*, No. 234–248.

[56] Hedlund, A., Evaluation of RANS Turbulence Models for the Simulation of Channel Flow; Teknisk-naturvetenskaplig Fakultet UTH-enheten: Upsala, Sweden, **2014**; p. 26.

[57] Davidson, L., An Introduction to Turbulence Models, Chalmers University of Technology: Goteborg, Sweden, **2018**.

[58] Bartosik, A., Simulation of a yield stress influence on Nusselt number in turbulent flow of Kaolin slurry, Proc. of the ASME Summer Heat Transfer Conf., **2016**, HTFEICNMM2016, No.2, pp. 1-7.

[59] Launder, B.E. and Sharma B.I., Application of the energy-dissipation model of turbulence to the calculation of flow near a spinning disc, *Letters in Heat and Mass Transfer*, **1974**, No.1 pp.131-138.

[60] Reynolds, O., On the dynamical theory on incompressible viscous fluids and the determination of the criterion, *Philosophical Transactions of the Royal Society of London*, **1895**, vol. 186, pp.123–164.

[61] Roache, P.J., Computational Fluid Dynamics, *Hermosa Publ., Albuquerque*, **1982**.

[62] Silva, R.C., Experimental characterization techniques for solid-liquid slurry flows in pipelines: A review, *Processes*, **2022**, vol. 10, No. 597, pp. 1-44.

[63] Javed, K., Vaezi, M., Kurian, V., Kumar, A., Frictional behaviour of wheat straw-water suspensions in vertical upward flows,

Biosystems Engineering, **2021**, vol. 212, pp. 30-45.

[64] DiCarlo, A. L., Holdsworth, D. W., Tamie L., Poepping, T.L., Study of the effect of stenosis severity and non-Newtonian viscosity on multidirectional wall shear stress and flow disturbances in the carotid artery using Particle Image Velocimetry, *Medical Engineering and Physics*, **2019**, vol.65, pp. 8–23.

Contribution of Individual Authors to the Creation of a Scientific Article (Ghostwriting Policy)

The author contributed to the present research at all stages from the formulation of the problem to the final findings and solution.

Sources of Funding for Research Presented in a Scientific Article or Scientific Article Itself

No funding was received for conducting this study.

Conflict of Interest

The authors have no conflict of interest to declare.